NASA Technical Memorandum 82797

Effect of Location in an Array on Heat Transfer to a Cylinder in Crossflow

Robert J. Simoneau and G. James Van Fossen, Jr.
Lewis Research Center
Cleveland, Ohio

Prepared for the
Third Joint Thermophysics Fluids, Plasma and Heat Transfer Conference
cosponsored by the American Institute of Aeronautics and
Astronautics and the American Society of Mechanical Engineers
St. Louis, Missouri, June 7-11, 1982

NASA

EFFECT OF LOCATION IN AN ARRAY ON HEAT TRANSFER TO A CYLINDER IN CROSSFLOW

by Robert J. Simoneau and G. James VanFossen, Jr.

National Aeronautics and Space Administration
Lewis Research Center
Cleveland, Ohio

E-1131

NOMENCLATURE

A	channel cross-section area, m^2
D	cylinder diameter, m
e_{rms}	root mean square of hot wire voltage fluctuation, volts
E	mean hot wire voltage, volts
I	heater current, amps
k	thermal conductivity, watts/m^2 K
L	cylinder length, m
Nu	Nusselt number (Eq. (2))
q	heat flux, watts/m^2
Re	Reynolds number (Eq. (1))
T	temperature, K
Tu	turbulence intensity (Eq. (3))
U	velocity, m/sec
V	heater voltage, volts
w	mass flow rate, kg/sec
y	distance across channel, m
μ	viscosity, N-sec/m^2

SUBSCRIPTS:

avg	average
b	bulk fluid conditions
o	no flow condition
w	wall

INTRODUCTION

The desire for increased gas turbine reliability and efficiency has stimulated research in all areas of turbine blade cooling. One widely used method of increasing the heat transfer to the coolant is to cast pin fins into the blade coolant flow passages. These pins must be relatively short because of passage size and manufacturing limitations. The large body of heat transfer data available for tube banks which is reviewed in Ref. 1 is not applicable to the turbine cooling case because the influence of the endwalls is not included (Endwalls are defined as the plane surfaces perpendicular to the pins that form the top and bottom of the flow channel.) Also in turbines the pins are usually quite short, less than four diameters. Recently, several experiments have been directed at this problem.

In Ref. 2 heat transfer and pressure drop results are presented for several geometries that model a turbine blade trailing edge. For these results a converging channel was used to simulate a turbine blade trailing edge cooling passage with pin length decreasing in the streamwise direction. However, high experimental uncertainty limits the usefulness of this work.

VanFossen (3) measured the average heat transfer coefficients for two four-row staggered arrays of short pin fins. The length-to-diameter ratios of the pins in the two arrays were 1/2 and 2. It was found that short pin fins increase the heat transfer significantly over that of the plain passage even though the 1/2 diameter long pins cover up as much endwall area as they add in pin surface area. It was also shown in Ref. 3 that the limited data available for pins as short as four diameters, from Refs. 4 and 5 are significantly different from the case of short pin fins.

In Refs. 6 and 7 the spanwise averaged heat transfer was measured for each row of pins for several staggered arrays of ten rows each. Heat transfer for short pins was found to be considerably lower than for long pins and the heat transfer increased in the streamwise direction for the first several rows until a peak was reached at about the third to fifth row. Heat transfer then decreased slightly in the streamwise direction. Reference 7 also showed that turbulence level, measured at a single point directly upstream of a given pin, was highest in the forward portion of the array and decreased to a lower level downstream.

The present work was performed concurrently with the work of Refs. 6 and 7 to gain some understanding of how array geometry and position within the pin array affects heat transfer to an individual pin. A single, heated pin was used to measure heat transfer in both staggered and in-line arrays. Length-to-diameter-ratio for all arrays was 3.01. Up to five rows of pins for both the staggered and in-line arrays were placed upstream of a row containing the heater transfer element. Turbulence intensity profiles across the channel, upstream of the heated pin, were measured for each configuration. Endwall heat transfer was not considered in this work.

This paper compares the various geometric configurations in terms of average Nusselt number over a Reynolds number range from 5,000 to 125,000. The results are discussed in terms of turbulence intensity profiles associated with each configuration.

DESCRIPTION OF EXPERIMENT

Apparatus

All of the tests were conducted using a rectangular flow channel 5.87 cm wide by 2.87 cm high. Pins, which were 0.953 cm in diameter (length-to-diameter ratio of 3.01) were installed in various array patterns. A typical pattern, four rows staggered, is shown in Fig. 1. The axial and transverse spacing were both 2.54 cm (spacing-to-diameter ratio of 2.67). Both staggered and in-line array patterns were used in configurations of one to six rows. The cover shown in Fig. 1 indicates the range of possible patterns. Only one cylinder was heated and that cylinder remained in a fixed position in the channel, as shown in Fig. 1. The various array patterns were achieved by adding or removing non-heated pins. For most of the tests the heated cylinder was in the last row in the array as shown. For a few tests two rows of pins were placed downstream of the heater. The pins touching the sidewalls of the channel had a small 0.083 cm flat machined on the side in order to fit the channel. The entrance to the channel was contoured as shown in Fig. 1.

The assembled channel with a given array pattern in place was subsequently installed in a cylindrical pressure chamber as part of a flow system which is shown schematically in Fig. 2. The flow system was a once-through system of pressurized nitrogen gas. The gas was lowered in pressure with a regulator and then passed through a calibrated metering orifice to a flow control valve, which further lowered the pressure and controlled the flow rate. The gas was then passed through a flow straightener, as shown in Fig. 2. The straightener, which was also used to reduce the inlet turbulence, had three elements. The first element was a wire screen with 0.23 mm diameter wire on a 16 mesh. The second was a honeycomb of plastic soda straws, approximately 0.64 cm diameter and 30 diameters long, while the third element was another screen which was the same as the first. This produced a turbulence intensity immediately ahead of the heated cylinder of about two percent. The test section pressure was controlled with two valves downstream in parallel for fine and course control. A range of pressures from 100 to 600 kPa were normally used; however, at the higher flow rates pressures below about 500 kPa were not possible. Finally, the flow was passed through a second calibrated metering orifice before being vented to the atmosphere. Because of the large pressure drop the gas temperature in the test section was low, ranging from 260 to 290 K.

Instrumentation

The heated cylinder was a commercial heater made of high resistance wire wound up and buried in a 0.953 cm diameter stainless steel tube. The tube wall thickness was approximately 0.080 cm. The heater was 3.81 cm long; thus approximately 25 percent of it extended into the channel walls. The heater was instrumented with eight chromel-constantan (type E) sheathed thermocouples buried in slots equispaced on the circumference. The thermocouple junctions were at the longitudinal midpoint of the cylinder with the orientation such that one was on the stagnation point. The power dissipated in the heater was measured using voltage taps on the power leads and a current shunt. The power source was a commercial SCR type DC power supply.

The flow system instrumentation is indicated on Fig. 2. Pressures were measured with strain gage transducers and temperatures were measured primarily with chromel-constantan thermocouples. The downstream orifice temperatures were measured with platinum resistance thermometers. The upstream orifice meter was used to measure the flow rate and the downstream orifice was used for redundancy. The upstream orifice static pressure could be varied from 300 to 6700 kPa. This allowed accurate metering over a 25 to 1 flow range with a single orifice plate and differential transducer.

The turbulence intensity measurements were made with a conventional temperature compensated hot film anemometer probe. The same probe was used for the entire experiment. The probe was a single element sensor traversed across the channel in front of the heated cylinder midway between it and the position of the first upstream row and at mid-channel height. The wire was aligned parallel to the cylinder axis. Position was measured with a linear potentiometer attached to the actuator.

All data except the turbulence measurements were recorded on the laboratory central data acquisition/mini-computer system, known as ESCORT (8) which provided real time updates at approximately two second intervals on a CRT. The mean and rms turbulence signals were recorded versus position on a two pen x-y recorder.

Data Reduction

The heat transfer data are presented in terms of standard Nusselt number versus Reynolds number plots. As will be discussed under RESULTS the data taken in this experiment did not support the use of the maximum velocity, based on minimum flow area, in computing the Reynolds number. The Reynolds numbers used herein are based on the mass flow rate and the channel cross-sectional area.

$$Re = \frac{wD}{\mu A} \tag{1}$$

The Nusselt number was computed on the basis of the total power dissipated divided by the exposed surface area of the heated cylinder.

$$Nu = \frac{qD}{(\Delta T)k} = \frac{(VI)}{\pi(T_{w,avg} - T_b)kL} \tag{2}$$

The wall temperature was the average of the eight surface thermocouples and the fluid temperature was measured at the inlet to the channel. A heat loss calibration was conducted with no flow and power to the heater. Over temperature differences from 6 to 40 K the calibration data normalized by Eq. (2) was constant at Nu ≈ 11. Thus all data presented herein have a loss correction of Nu = 11 subtracted from the raw data.

The thermophysical properties used in Eqs. (1) and (2) were all calculated at the inlet temperature. The density was calculated on the basis of ideal gas. The viscosity and thermal conductivity were simple curve fits to the data of Ref. 9.

The turbulence data were all acquired using an uncalibrated temperature compensated probe, since the operating conditions were well below room temperature. The temperature compensated probe was used merely to minimize drift. Since the primary interest was to make relative comparisons, this was considered adequate. For uncalibrated probes it is possible to derive an approximate linearized expression for turbulence intensity (10-11).

$$Tu = \frac{4E\ e_{rms}}{(E^2 - E_o^2)} \times 100 \tag{3}$$

Equation (3) was used for all turbulence data.

RESULTS

Heat Transfer

The experiment was conducted over a Reynolds number range from 5,000 to 125,000. The fluid temperature ranged from 260 to 290 K and the surface to fluid temperature difference from about 20 to 40 K. The system pressure ranged from 100 to 600 kPa. In general the higher flow rates resulted in higher pressures and vice-versa; however, the back pressure was frequently and randomly varied to insure that there was no systematic pressure effect. This was important because changing pressure at a given Re really meant changing velocity.

Two reference cases are presented in Figs. 3 and 4. The data of Fig. 3 were taken with only the heated cylinder in the channel, while Fig. 4 is for data with a single row containing the heated cylinder. The latter case is referred to as a one row array. In both cases the data plotted were taken on three separate days spanning time from the beginning of the total experiment to the end. The results show good repeatability. The correlations presented by Kreith (12) of Hilpert's data for average heat transfer to a cylinder in crossflow are included on Figs. 3 and 4 as a reference.

The first observation is that the two cases are not much different, especially at the lower Reynolds numbers. The one row case is above the heater-only case by seven percent at Re = 10^4 and 15 percent at Re = 10^5. The ratio of the two maximum velocities based on flow blockage for these cases is 1.55. It is clear that the small difference is not a direct result of flow blockage and for this data the maximum velocity is not the correct choice for computing Reynolds number. The one row data follow the general trend of Hilperts data (12) even exhibiting a change in slope. The data of Fig. 4 will be the base reference for all the rest of the data.

No correlating equations will be presented in this paper because the authors feel the results are too geometry specific to have widespread application. It is encouraging, however, that data follow the general trends exhibited by Hilperts data. The slope of the high Re data is 0.80 and the low Re data is 0.58. The two percent turbulence intensity level (even higher near the walls) was probably higher than in Hilperts case which could explain the higher heat transfer levels. Further, although blockage does not have a one-to-one effect, it does increase heat transfer, as shown by comparing Figs. 3 and 4.

Although the heavy cylinder wall yielded an approximately isothermal surface, there was a small circumferential temperature gradient (2 to 4 K). This pattern varied over the Reynolds number range. At high Re the temperature increased from its lowest value at the stagnation point to about the 90° point, then decreased to a value at 180° which was near the stagnation value. At low Re the increase in temperature continued well past the 90° point with highest value frequently being at the rear of the cylinder. Usually slope changes in the data were accompanied by changes in the circumferential temperature pattern.

Heat transfer data obtained from two to six row arrays are presented in Fig. 5 for the in-line pattern and in Fig. 6 for the staggered pattern. The row containing the heater pin is always the last row. A mean line from the one row data of Fig. 4 is included for reference and is labeled base case. Three results stand out distinctly in these data. First, the addition of cylinders upstream of the heated cylinder in either pattern significantly increases heat transfer. Second, for the in-line arrays the number of upstream rows has little or no effect on the heat transfer level whereas for the staggered arrays the heat transfer level is definitely affected by the number of upstream rows. Finally, the rather strong knee that exists in the one row base case and in Hilpert's data does not appear in the multiple row data. Slight slope changes do occur but nothing as strong or consistent as the reference cases.

In order to facilitate comparison, mean lines of all the data, without symbols, are plotted together on Fig. 7. In producing Fig. 7 each array case was plotted separately and a best fit straight line was drawn through the data. The in-line data actually showed slight (three percent) level differences but no pattern was exhibited. A single line is shown, since these differences were within experimental error. The staggered array data exhibit level differences from row to row. Relative to the

one row case, the average increase in heat transfer for two to six row arrays was 21, 64, 58, 46, and 46 percent respectively. The in-line results had an average heat transfer increase of 80 percent over the one row base case. The maximum that occurs for a three row array in the staggered pattern was seen also by Metzger and co-workers (6-7). Level comparisons with Metzger, et al., are not appropriate since their data included heat transfer from the endwalls. Zukauskas (1) presents some data for four row arrays in both in-line and staggered patterns, presumably long tubes. There is not enough information for a direct comparison, however, Zukauskas' data show an increase in heat transfer of four rows over one row of 40 and 59 percent for in-line and staggered arrays respectively. In addition to level the staggered arrays show variations in slope of 0.63, 0.62, 0.59, 0.60 and 0.60 for two to six rows respectively. The in-line data had a fairly constant slope of 0.66.

Since in the present experiment the instrumented row was fixed in the channel and the array pattern was changed for each run, a few tests were performed where two rows of pins were added downstream of the row containing the heater. Two cases were run for each pattern. One was the no upstream row case, making the heater row the first in a three row array. The other was the three rows upstream case, making the heater row fourth in a six row array. The results are shown in Fig. 8 for the in-line pattern and in Fig. 9 for the staggered pattern. On each figure the one row base case is drawn as a solid line and the three row upstream no rows downstream case is drawn as a dashed line. The first result to observe is that for either pattern, if the row of interest is embedded in an array (i.e., three rows upstream), the addition of rows downstream had no effect on the heat transfer. If, however, the row of interest is the first row then as can be seen there is a difference whether or not there are downstream rows. Additional data points were taken in the regions where deviations from the base occurred. The results appears both real and stable. Variations appeared in the circumferential temperature patterns. Some type of transition seemed to be occurring. It seems reasonable that the downstream pins are affecting the flow around the heated cylinder, possibly affecting separation. What seems strange is that the results are fairly similar for both the in-line and staggered arrays.

Turbulence

Turbulence intensity profiles were measured for each configuration discussed in the heat transfer results. They were measured at nominal Reynolds numbers of 10,000, 50,000, and 120,000 for each configuration. The heater was not powered during these runs. Since it would be impossible to show all the data, representative samples are shown in Figs. 10 to 13. The array pattern is sketched on the figures as a visual reference. In all cases the probe traverses from left to right across the figure.

The first case, Fig. 10, is the one row base case at the three Reynolds numbers. In general the turbulence intensity over two-thirds of the channel approaching the first row is about two percent. The data of Fig. 10 was repeated several times. The spike in the Re = 120,000 case repeats and appears to occur as the thickest part of the hot wire probe passes in front of the center cylinder, as it moves from left to right. This is probably the probe body wake interacting with the heated cylinder. The small turbulence increases on left are also repeatable and are probably not a probe influence but it cannot be said for sure, since the thick part of the probe is already in the channel at this point.

Figure 11 are intensity profiles at Re = 50,000 for the two to six row arrays in the in-line pattern. The heat transfer result, which showed no influence of adding rows upstream, is very consistent with the turbulence intensity profiles. Only the two row array (one row upstream) shows any difference. It shows a higher peak in the cylinder wake and lower intensity between the cylinders. Apparently a fully developed flow condition has not yet been reached. The average intensity may well be equivalent to the fully developed (three rows and greater) value. The fact that the one row upstream in-line heat transfer values are the same as the rest could be fortuitous. Obviously, though, by two rows upstream for the in-line case the flow is fully developed and a channel between the cylinders is formed.

Figure 12 displays the intensity profiles at Re = 50,000 for the two to six row arrays in the staggered array. Again, the turbulence intensity profiles, which exhibit a maximum in intensity in the range of two to three rows upstream of the heated cylinder, are consistent with the heat transfer results. Since the staggered array is an alternating pattern, the profiles are more complex, but in general the row immediately upstream of the heated row has a major influence. Since the profile shape is changing, the row causing maximum average intensity is not clear, but it is either the second or third upstream. After three rows the intensity was clearly decreased as was the heat transfer. The heat transfer appears to level off but the intensity is still decreasing, with five rows upstream. Metzger's results (6-7) suggest a leveling off by five rows.

An overlay of Figs. 11 and 12 shows that, although the profile shapes are quite different, the average turbulence intensity for both cases is similar at about 25 percent. Similarly the average increase in heat transfer for either pattern is about 50 percent. One would suspect that these numbers would change as the spacing is changed.

Finally, to examine the effect of Reynolds number the intensity profiles for three Reynolds numbers are shown in Fig. 13 for the four row staggered array. The average turbulence intensity decreases with increasing Reynolds number. The profiles also tend to flatten out more in front of the heated cylinder as the Reynolds number increases. Thus for the four row array there is less turbulence at high Re than at low Re. This may explain the tendency of the heat transfer to increase more slowly with Re in the four row array than in the one row base case, where there is little effect of Re on turbulence level.

In general, it would appear that the heat transfer results are very consistent with and explainable in terms of the turbulence intensity profiles.

SUMMARY AND CONCLUSIONS

1. There was very little difference in the heat transfer levels for the case with only the heater in the channel and the case with the heater and two dummy pins across the channel despite a 55 percent difference in open area. This suggests that average channel velocity is a more appropriate reference than maximum velocity.

2. The base reference case for all configurations was one row containing the heater and two dummy pins. This base case followed the general trend of the data in the literature for heat transfer to a cylinder in crossflow at about a 25 percent higher level.

3. Addition of cylinders upstream in an in-line array pattern, one to five rows, produced an average of about 50 percent increase in heat transfer level above the base case. The number of upstream rows had little or no influence.

4. The turbulence intensity profiles for the in line arrays were virtually identical for the cases of two to five upstream rows. The intensity varied from a peak of about 46 percent in the wake (i.e., channel centerline) to an average of about ten percent between the cylinders. The one row upstream case was somewhat different, exhibiting a higher peak and lower midchannel value.

5. Addition of cylinders upstream in a staggered array pattern produced average increases in heat transfer of 21, 64, 58, 46, and 46 percent above the base case for one to five rows respectively.

6. The turbulence intensity profiles for the staggered arrays were different for each case, one to five rows. In general, the average intensity first increased then decreased with the addition of upstream rows of cylinders. This behavior of the turbulence intensity is reflected in the heat transfer results.

7. The addition of cylinders downstream of the heater row in either array pattern had no effect on the heat transfer results due to upstream rows. It had some influence on the base case.

8. While the specific heat transfer results are only applicable to the short pin cases commonly found in turbine blades, the observations on the turbulent wake profiles and their influence on heat transfer should be applicable to broader cases of tube banks.

REFERENCES

1 Zukauskas, A., "Heat Transfer from Tubes in Crossflow," Advances in Heat Transfer, Vol. 8, J. P. Hartnett and T. F. Irvine, Jr., eds., Academic Press, 1972, pp. 93-160.

2 Brown, A., Mandjikas, B., and Mudyiwa, J. M., "Blade Trailing Edge Heat Transfer," ASME Paper No. 80-GT-45, Mar. 1980.

3 VanFossen, G. J., "Heat Transfer Coeffi cients for Staggered Arrays of Short Pin Fins," ASME Paper No. 81-GT-76, Mar. 1981.

4 Kays, W. M., and London A. L., Compact Heat Exchangers, National Press, Palo Alto, Calif., 1955.

5 Theoclitus, G., "Heat Transfer and Flow Friction Characteristics of Nine Pin Fin Surfaces," Journal of Heat Transfer, Vol. 88, No. 4, Nov. 1966, pp. 385 390.

6 Metzger, D. E., Berry, R. A., and Bronson, J. P., "Developing Heat Transfer in Rectangular Ducts with Arrays of Short Pin Fins," presented at the 1981 ASME Winter Annual Meeting, Washington, DC, ASME Paper 81-WA/HT-6.

7 Metzger, D. E., and Haley, S. W., "Heat Transfer and Flow Visualization for Arrays of Short Pin Fins," presented at the 1982 ASME Gas Turbine Conference, London, ASME paper 82-GT-138.

8 Miller, R. L., "ESCORT: A Data Acquisition and Display System to Support Research Testing," NASA TM-78909, May 1978.

9 Hilsenrath, J., et al., "Tables of Thermal Properties of Gases," NBS Circular 564, Nov. 1955.

10 "Hot Wire and Hot Film Measurements and Applications," Thermal Systems, Inc., Technical Bulletin No. 4, p. 35.

11 Bearman, P. W., "Corrections for the Effects of Ambient Temperature Drift on Hot Wire Measurements in Incompressible Flow," DISA Information Bulletin No. 11, May 1971, p. 26.

12 Kreith, F., Principles of Heat Transfer, 2nd ed., International Textbook Company, Scranton, PA, 1966.

ORIGINAL PAGE
BLACK AND WHITE PHOTOGRAPH

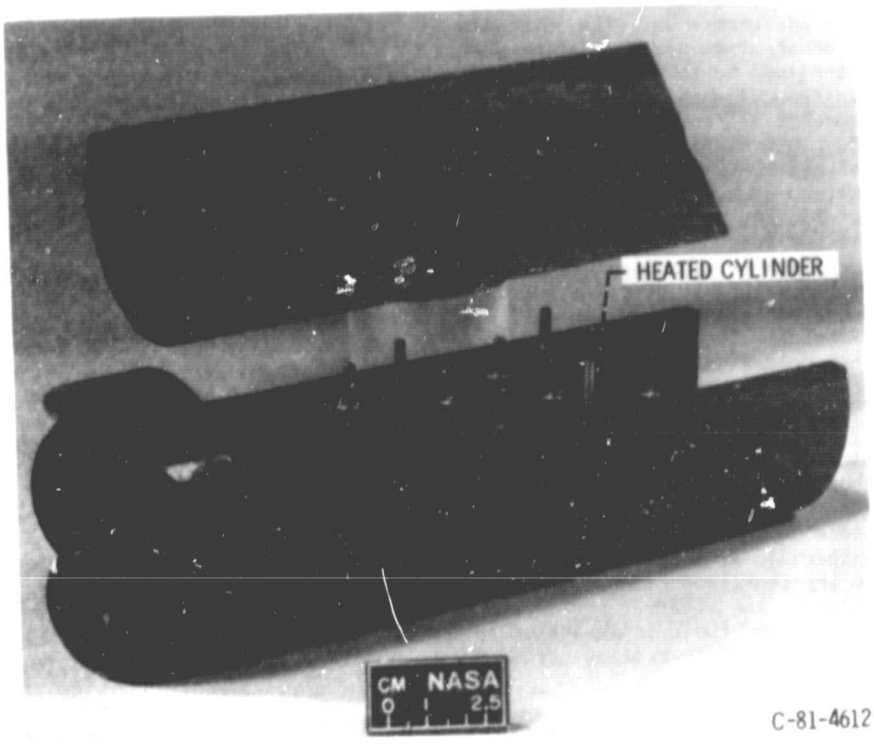

C-81-4612

Figure 1. - Photograph of test section channel with four row staggered array in place.

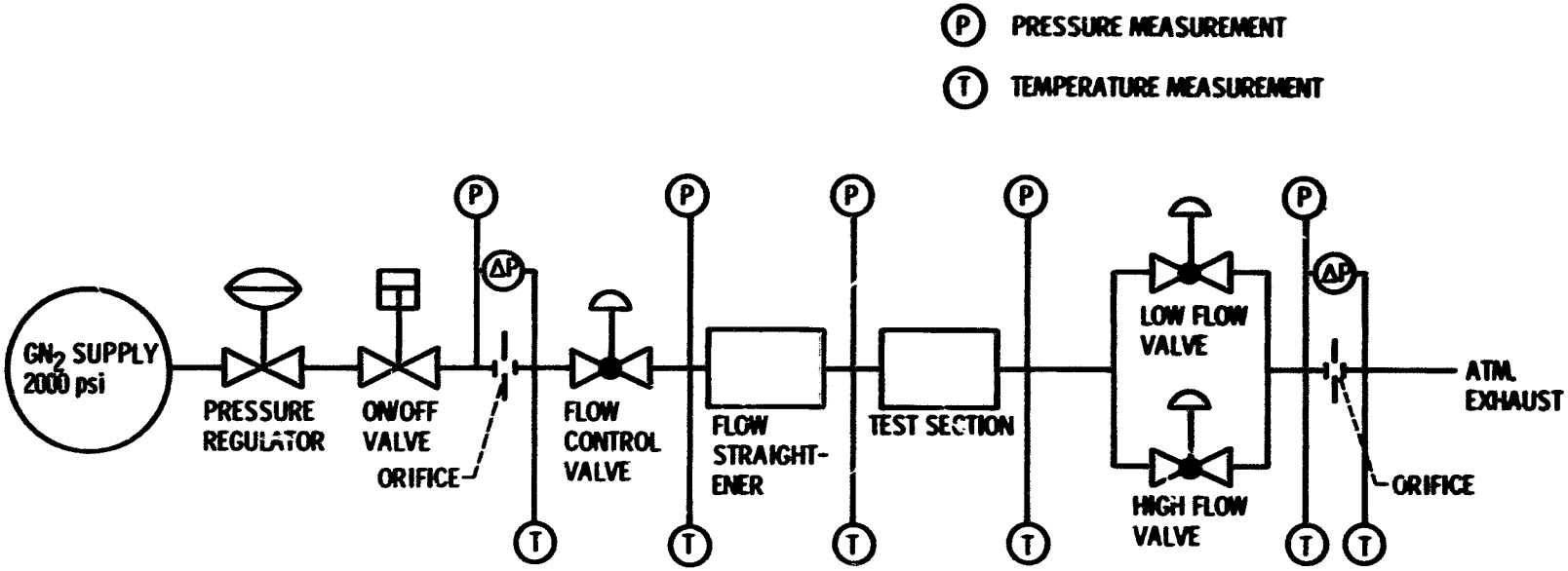

Figure 2. - Flow schematic for pin wake heat transfer experiment.

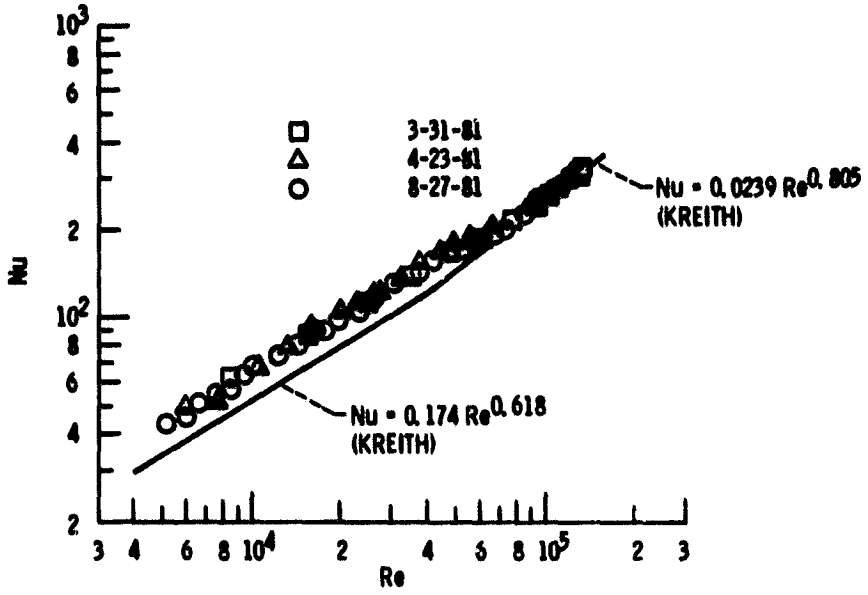

Figure 3. - Heat transfer with heater only - no unheated pins - in channel.

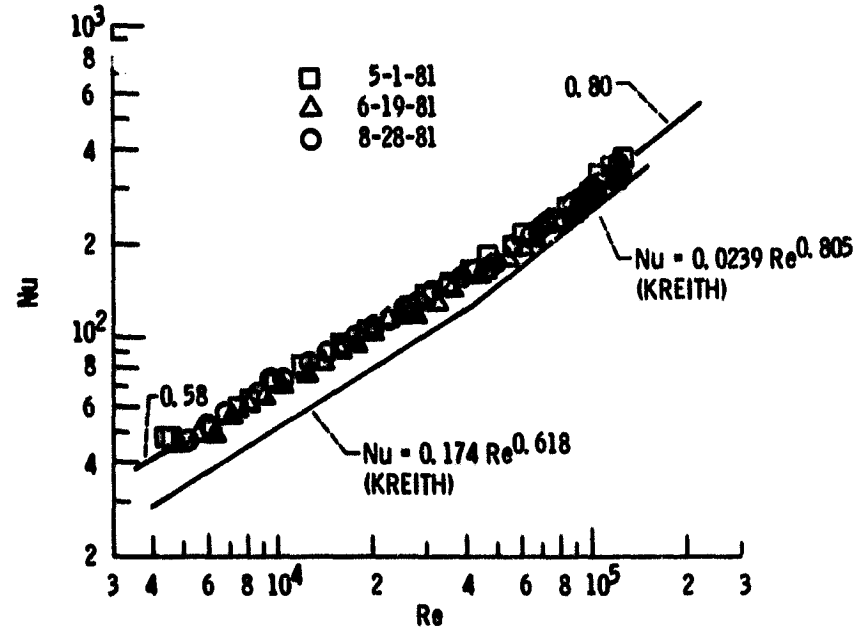

Figure 4. - Heat transfer with one row in channel - base case.

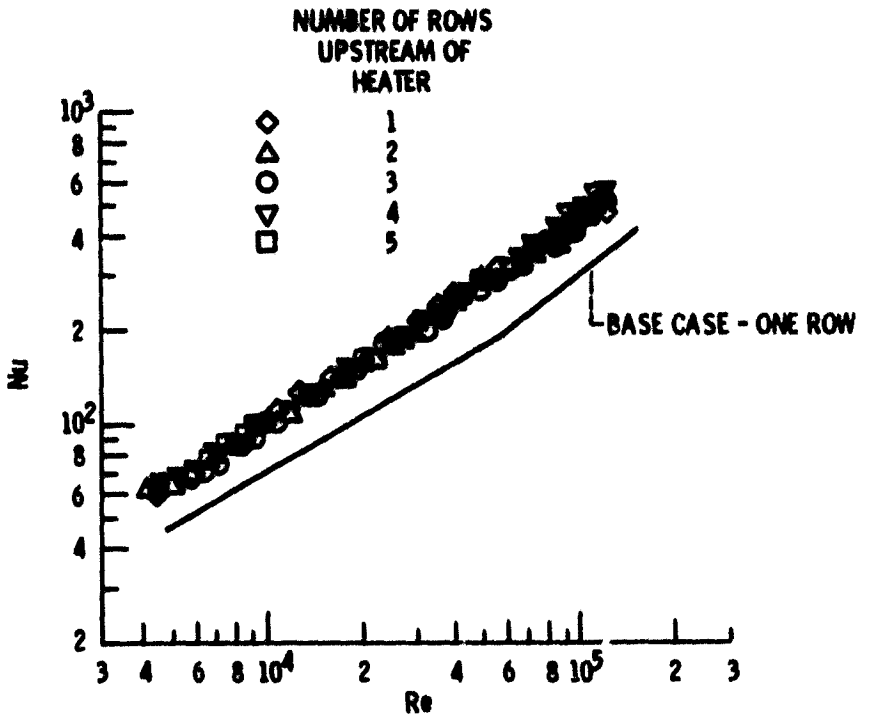

Figure 5. - Heat transfer in two to six row arrays with in-line pattern.

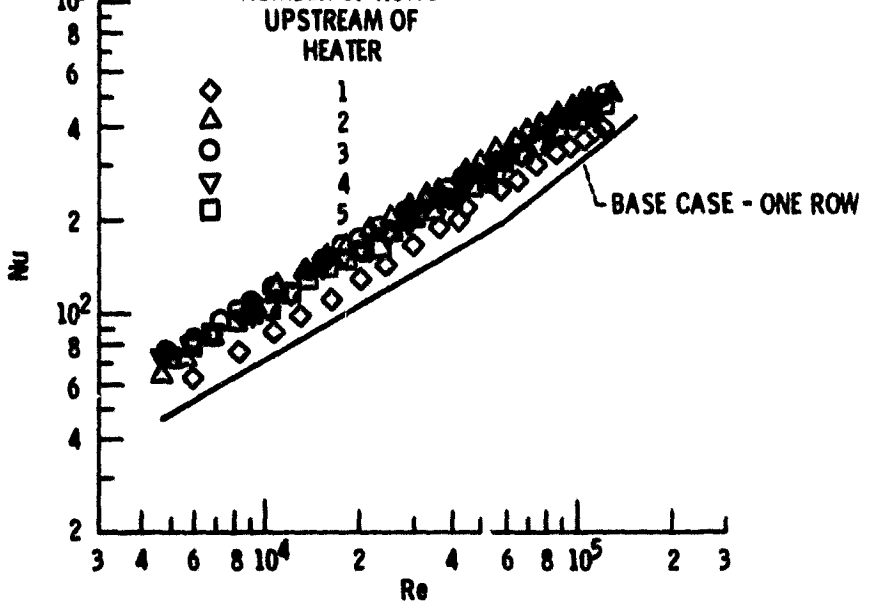

Figure 6. - Heat transfer in two to six rwo arrays with staggered pattern.

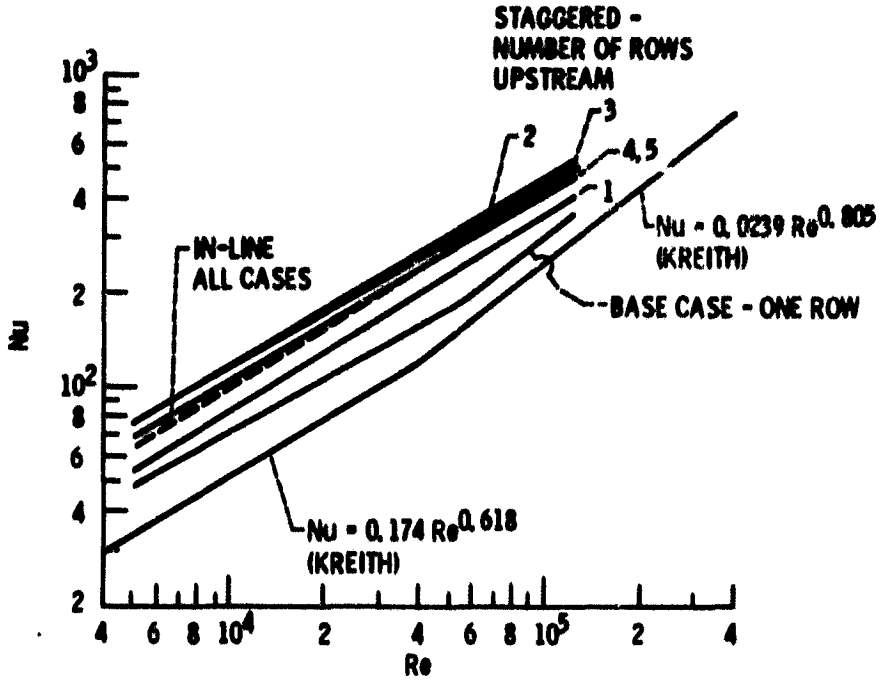

Figure 7. - Summary of data.

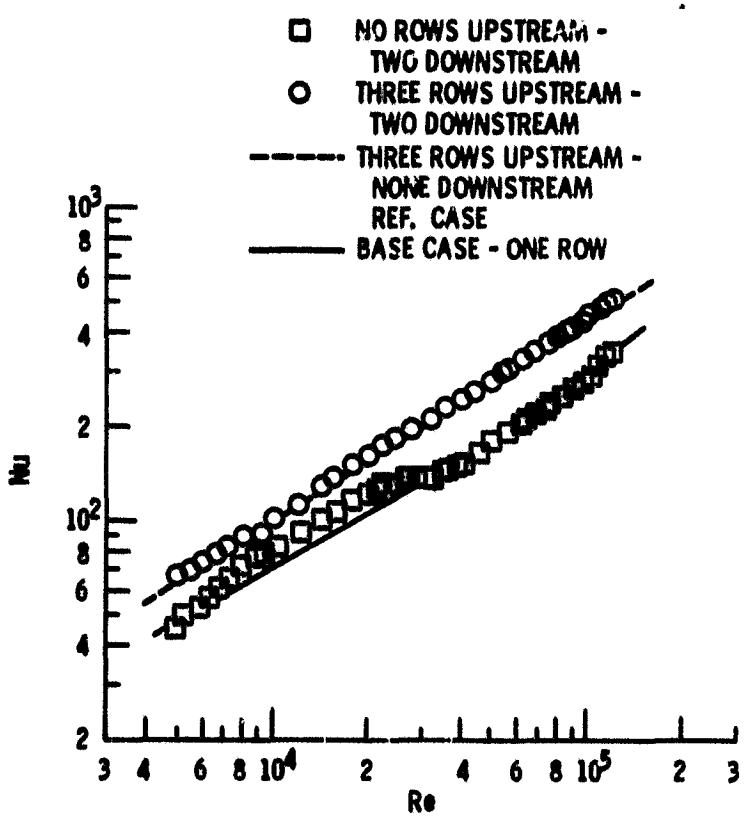

Figure 8. - Effect of adding two rows downstream - in-line pattern.

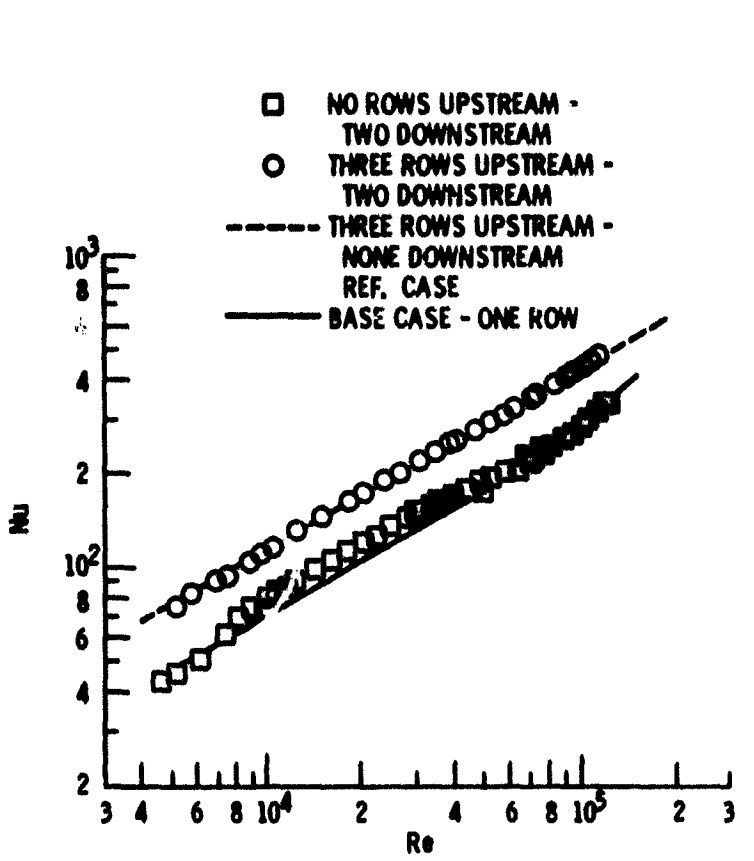

Figure 9. - Effect of adding two rows downstream - staggered pattern.

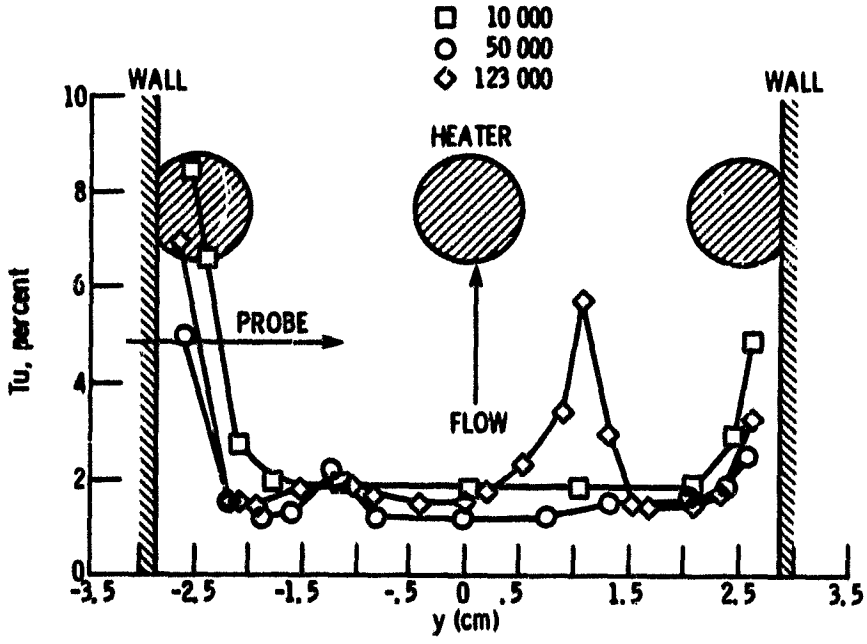

Figure 10. - Turbulence intensity for one row array (no upstream disturbance) at several Reynolds numbers.

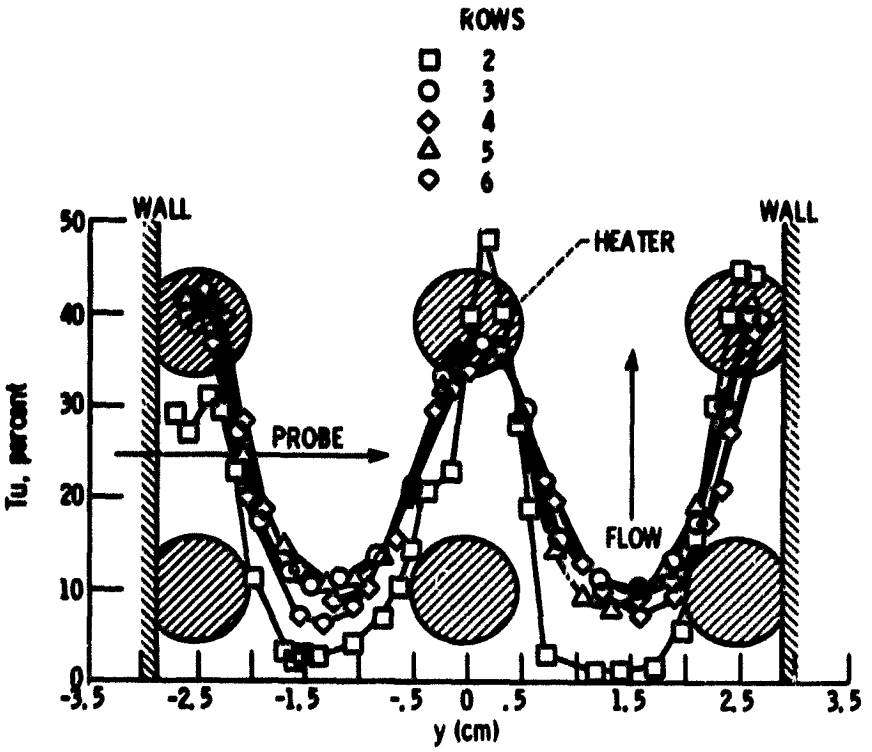

Figure 11. - Turbulence intensity profiles for two to six row arrays with in-line pattern at nominal Re = 50 000.

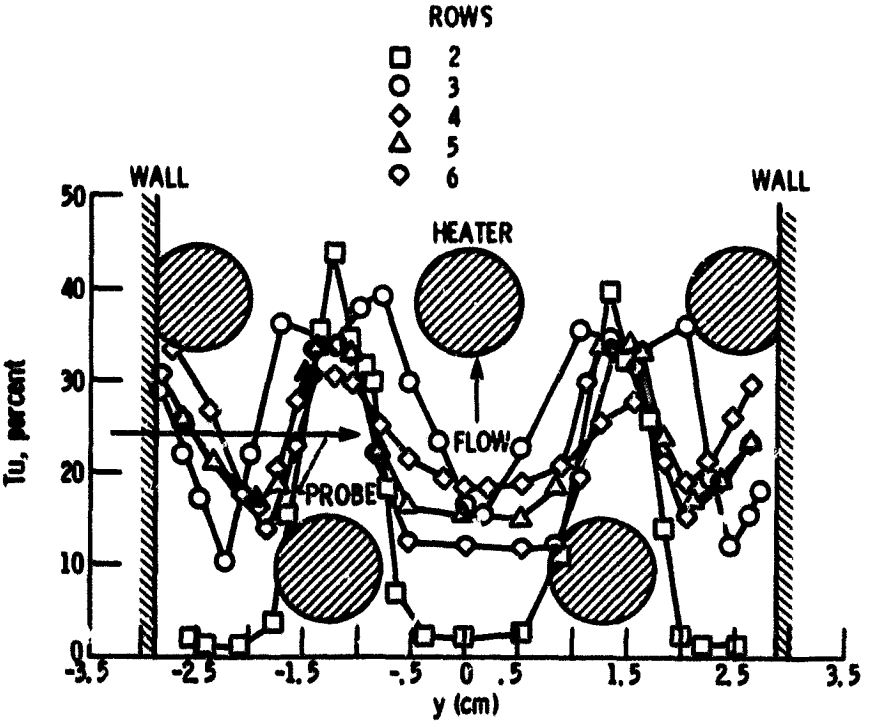

Figure 12. - Turbulence intensity profiles for two to six row arrays with staggered pattern at nominal Re = 50 000.